

CO2 Absorption and Regeneration Cycling with Micro-Encapsulated CO2 Sorbents (MECS)

J. M. Knipe, K. P. Chavez, K. M. Hornbostel, M. A. Worthington, D. T. Nguyen, C. Ye, W. L. Smith, S. E. Baker, J. F. Brennecke, J. K. Stolaroff

February 24, 2018

Environmental Science & Technology

Disclaimer

This document was prepared as an account of work sponsored by an agency of the United States government. Neither the United States government nor Lawrence Livermore National Security, LLC, nor any of their employees makes any warranty, expressed or implied, or assumes any legal liability or responsibility for the accuracy, completeness, or usefulness of any information, apparatus, product, or process disclosed, or represents that its use would not infringe privately owned rights. Reference herein to any specific commercial product, process, or service by trade name, trademark, manufacturer, or otherwise does not necessarily constitute or imply its endorsement, recommendation, or favoring by the United States government or Lawrence Livermore National Security, LLC. The views and opinions of authors expressed herein do not necessarily state or reflect those of the United States government or Lawrence Livermore National Security, LLC, and shall not be used for advertising or product endorsement purposes.

"Evaluating the Performance of Micro-Encapsulated CO₂ Sorbents during CO₂ Absorption and Regeneration Cycling"

Knipe, Jennifer M.¹, Chavez, Kathya P.²,

1

2

5

6

7

8

9

10

11

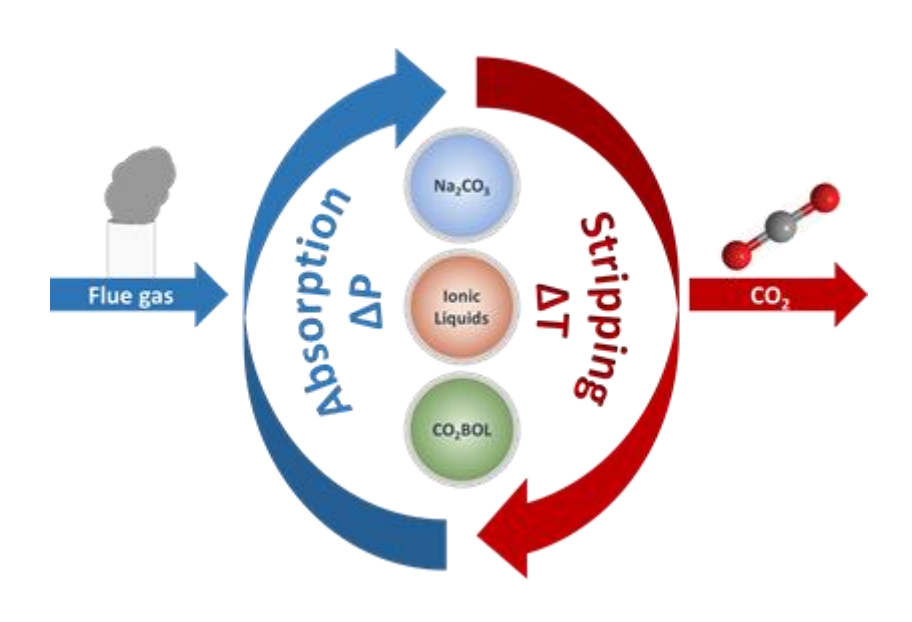
Knipe, Jennifer M.¹, Chavez, Kathya P.², Hornbostel, Katherine M.³, Worthington, Matthew A.¹,

Nguyen, Du T. 1, Ye, Congwang 1, Bourcier, William L. 1, Baker, Sarah E. 1, Brennecke, Joan F. 4,

Stolaroff, Joshuah K.*1

1 Lawrence Livermore National Laboratory, 2 University of Illinois at Chicago, 3 University of

Pittsburgh, 4 The University of Texas at Austin



12 Abstract: We encapsulated six solvents with novel physical and chemical properties for CO₂ 13 sorption within gas-permeable polymer shells, creating Micro-Encapsulated CO₂ Sorbents 14 (MECS), to improve the CO₂ absorption kinetics and handling of the solvents for post-combustion 15 CO₂ capture from flue gas. The solvents were sodium carbonate (Na₂CO₃) solution, uncatalyzed 16 and with two different promoters, two ionic liquid (IL) solvents, and one CO₂-binding organic 17 liquid (CO₂BOL). We subjected each of the six MECS to multiple CO₂ absorption and regeneration 18 cycles and measured the working CO₂ absorption capacity as a function of time to identify 19 promising candidate MECS for large-scale carbon capture. We discovered that the uncatalyzed 20 Na₂CO₃ and Na₂CO₃-sarcosine MECS had lower CO₂ absorption rates relative to Na₂CO₃-cyclen 21 MECS over 30 minutes of absorption, while the CO₂BOL Koechanol appeared to permeate 22 through the capsule shell and is thus unsuitable. We rigorously tested the most promising three 23 MECS (Na₂CO₃-cyclen, IL NDIL0309, and IL NDIL0230) by subjecting each of them to a series 24 of 10 absorption/stripping cycles. The CO₂ absorption curves were highly reproducible for these 25 three MECS across 10 cycles, demonstrating successful absorption/regeneration without 26 degradation. As the CO₂ absorption rate is dynamic in time and the CO₂ loading per mass varies 27 among the three most promising MECS, the process design parameters will ultimately dictate the 28 selection of MECS solvent.

1. Introduction

29

- 30 Global carbon dioxide emissions are projected to continue increasing in the near term, with coal-31 consuming countries such as China and India contributing to the expected growth over the next 32 several years. The rate of increase in anthropogenic CO₂ emissions more than doubled in the 33 period from 2000–2014, to 2.5–2.7% per annum, relative to the 1.1% per annum increase in the 1990–1999 period.^{2,3} The concentration of CO₂ in the atmosphere now exceeds 400 ppm, the 34 highest it has been in 670,000 years. ⁴ The increasing global anthropogenic CO₂ emissions presents 35 a challenge to meet the international target of <2°C increase in global temperature relative to pre-36 37 industrial levels. Thus, investigating carbon capture, storage, and utilization strategies is critical to 38 mitigating CO₂ emissions and maintaining <2°C global temperature increase.
- 39 Globally, the combustion of fossil fuels accounts for 75% of anthropogenic CO₂ emissions.² In 40 2016, 35% of the US energy-related CO₂ emissions came from the electric power sector fed by 41 fossil fuels.⁵ One strategy for CO₂ emission mitigation is post-combustion capture of CO₂ from 42 point-sources such as power plants. The conventional approach to CO₂ capture from flue gas is 43 amine-scrubbing using aqueous solutions of amines such as monoethanolamine (MEA) or 44 diethanolamine (DEA), which is already used in a number of plants but suffers from high energy 45 demand, mostly to regenerate the amine solvent, as well as degradation of the amine solvent and the formation corrosive degradation products.^{6,7} These challenges limit the economic feasibility of 46 47 post-combustion CO₂ capture from powers plants. Therefore, developing novel CO₂ sorbents and 48 processes that reduce the energy requirement and/or increase the CO₂ absorption rate is a vital area 49 of research to meet CO₂ emissions and global temperature goals.

50 For example, Heldebrandt and coworkers have developed CO₂ binding organic liquids (CO₂BOLs) 51 that increase the CO₂ absorption capacity and reduce the required regeneration temperature from 120°C to 75°C when coupled with the polarity-swing-assisted regeneration (PSAR) process.^{8,9} 52 53 Brennecke and coworkers have developed ionic liquids (ILs) with tunable CO2 capacity and regeneration energy^{10–13} as well as phase-change ILs¹⁴ that utilize the heat of fusion to reduce the 54 55 energy requirement for regeneration. However, several of the recently developed novel, advanced 56 solvents for CO₂ absorption suffer from limitations such as high viscosity, poor diffusion of CO₂, 57 equipment fouling, or difficult separation of the CO₂-loaded sorbent, so different operational 58 strategies must be developed for their use.

Micro-Encapsulated CO₂ Sorbents (MECS) are a recently-developed CO₂ capture technology that may be an effective strategy for enabling the use and recyclability of advanced solvents, but they have not been rigorously evaluated for practical use within an absorption/regeneration process until now. MECS consist of a CO₂-absorbing solvent or slurry encased in spherical, CO₂-permeable polymer shells. 15,16 We have demonstrated this technology with carbonates, CO₂BOLs, and ionic liquids to achieve increased surface area, resulting in an enhancement of CO₂ absorption rates by an order of magnitude relative to a thin film of the solvent.¹⁶ CO₂ promoters such as carbonic anhydrase¹⁷, sarcosine¹⁸, or zinc (II) cyclen complexes^{19,20} may be combined with carbonate solutions in MECS to further increase the rate of CO₂ absorption. We have previously explored the addition of zinc (II) cyclen, a mimic of the enzyme carbonic anhydrase that catalyzes CO₂ absorption into aqueous solution, to carbonate MECS to enhance the rate of CO₂ absorption and found that the capsules reached CO₂ saturation 2-3 times faster than carbonate MECS without cyclen. 15 Here, we rigorously demonstrate successful encapsulation, compare absorption rates and capacities of CO₂ at low partial pressure, and evaluate stability of six advanced liquid CO₂ solvents within polymer shells: Na₂CO₃ solution (uncatalyzed, with sarcosine, with cyclen); ionic liquids (task specific ionic liquid NDIL0230, and phase-changing ionic liquid NDIL0309), and a CO₂BOL (Koechanol). We build upon our previous encapsulation tests to characterize MECS performance over a wider range of temperatures, CO₂ loadings, and absorption/regeneration cycles.

2. Methods

59

60

61

62

63

64

65

66

67 68

69

70

71

72

73

74

75

76

77

78 Six MECS formulations were prepared for CO₂ absorption experiments, as summarized in Table 1. Three variations of sodium carbonate (17% Na₂CO₃ by weight) MECS were manufactured: 79 Na₂CO₃ with 0.2 sodium bicarbonate loading, Na₂CO₃ with 50 mM cyclen catalyst¹⁵ and 0.05 wt% 80 81 alumina, and Na₂CO₃ with 600 mM promoter amino acid sarcosine and 0.2 sodium bicarbonate loading. 18 Sodium carbonate, sodium bicarbonate, sarcosine, and potassium hydroxide were 82 83 purchased from Sigma-Aldrich (St. Louis, MO). The sarcosine was first deprotonated to its active 84 salt form with potassium hydroxide, then lyophilized and used to prepare core solutions for 85 capsules. The pH of the sodium carbonate solutions was titrated to ~11.2. In addition to the three 86 Na₂CO₃ MECS types, two ionic liquid solvents were encapsulated and tested. Both are proprietary 87 compounds developed for CO₂ capture, and provided by the Brennecke group at the University of Notre Dame and The University of Texas at Austin (USA). They are designated NDIL0309, a 88

phase-changing IL, and NDIL0230. The CO₂BOL MECS were prepared with Koechanol provided by Heldebrandt and coworkers at Pacific Northwest National Laboratory (USA). All MECS capsules were prepared by a double-emulsion microfluidic technique as described previously. ^{15,16} Briefly, MECS were created by flowing solvent core and polymer shell material in an inert carrier fluid through a microfluidic junction to create a double emulsion of solvent cores within polymer shells, suspended in carrier fluid. The MECS are then cured by brief exposure to ultraviolet light. The carbonate and Koechanol MECS were prepared with commercial silicone Tegorad 2650 (Evonik Industries AG, Essen, Germany) shell material, and the ionic liquid MECS were prepared with a custom silicone shell material designated thiolene-Q. ¹⁶ The permeability of each silicone to nitrogen and CO₂ was measured using a constant-volume, differential-pressure apparatus, in which pressure sensors on either side of the silicone membrane measure the rate of pressure change, or 'leak-up' rate, as the gas moves from the high pressure volume, through the membrane and into the low pressure volume, as described previously. ¹⁵

CO₂ absorption rates were measured by distributing a thin layer (monolayer when possible) of MECS on a wire mesh or within a wire mesh enclosure in a sealed apparatus with pressure transducer (Omega, 0.08% BSL error) and a jacketed, temperature-controlled chamber $(\pm 1.5^{\circ}\text{C})^{15}$, shown schematically in Figure 1. In the case of sodium carbonate MECS, which contained aqueous solution, 2.5 ml of water was included in the chamber for experiments run at temperatures greater than 25°C to prevent the capsules from dehydrating. In these cases, a background of CO₂ absorption by 2.5 ml of water was subtracted from the absorption by the carbonate MECS. The air in the chamber was evacuated to ~0.01 bar, then the valve was closed and the chamber was given ~10 minutes to reach equilibrium pressure due to water vapor formation. The chamber was then filled with CO₂ to a desired partial pressure of CO₂ (typically 0.1 bar to simulate flue gas). The pressure within the chamber was then measured at a sampling frequency of 10 s⁻¹ over the course of ~1 hour. CO₂ loading was then determined as a function of cumulative pressure drop, according to the governing equation:

$$L_{CO_2} \equiv \frac{n_{CO_2}}{m_{sol}} = \frac{\Delta PV}{m_{sol}RT} \tag{1}$$

where CO_2 loading, L_{CO_2} , is defined as the total CO_2 absorbed by the MECS, n_{CO_2} [mol], per mass of core solvent in the sample, m_{sol} [kg]. The mass of the core solvent was determined based on the flowrates and densities of the core and shell materials during fabrication in the microfluidic device. According to the ideal gas law, this ratio can be expressed in terms of the cumulative pressure drop in the chamber, ΔP , which is equivalent to the CO_2 partial pressure drop, since water vapor partial pressure is already in equilibrium before CO_2 is introduced. Thus, CO_2 loading is measured over the course of at least 30 minutes for each capsule sample and normalized by solvent mass to compare CO_2 absorption rates and capacities for the six MECS types. The CO_2 uptake by the silicone material alone was measured to be <0.1% of the total CO_2 uptake by MECS; as the uptake by silicone is negligible, we have not subtracted it as background.

126 The stoichiometric capacity was calculated by:

$$\frac{\text{moles CO}_2 \text{ absorbed}}{\text{total moles solvent}} \chi \ 100\% \tag{2}$$

where the solvent is Na₂CO₃, NDIL0309, or NDIL0230.

The CO₂ absorption rate was calculated by taking the time step derivative of the loading curve of micromoles of CO₂, normalizing by the total mass of MECS [g] and the partial pressure of CO₂ [bar] at each time step, and applying a smoothing function, a fast Fourier transform filter over 500 points using Origin data analysis software.

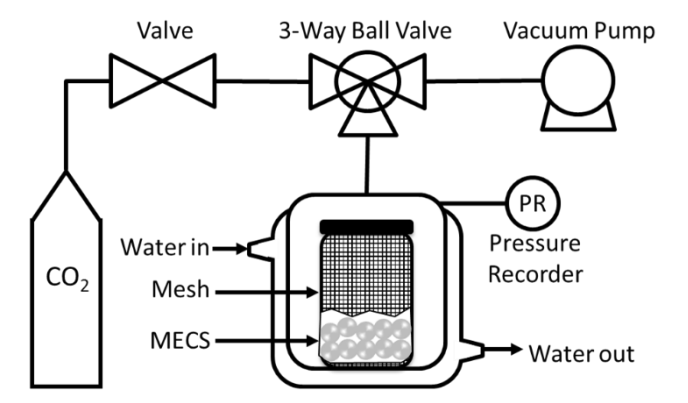


Figure 1: Process diagram of the pressure drop apparatus used to measure CO₂ absorption rates as a function of time for all six MECS types.

In the preliminary tests, MECS were cycled by thermal regeneration in a 50 mm diameter tube furnace at 130°C under flow of nitrogen for 1 hour, shown schematically in Figure 2A. All carbonate MECS were regenerated with nitrogen bubbled through water at 100°C and a reservoir of water was included with the MECS to help prevent dehydration. The MECS were regenerated for an hour, then immediately removed from the furnace, weighed, and placed in the chamber of the pressure drop setup to measure CO₂ absorption. During tube furnace regeneration, the MECS lost as much as 60% of their mass due to water loss.

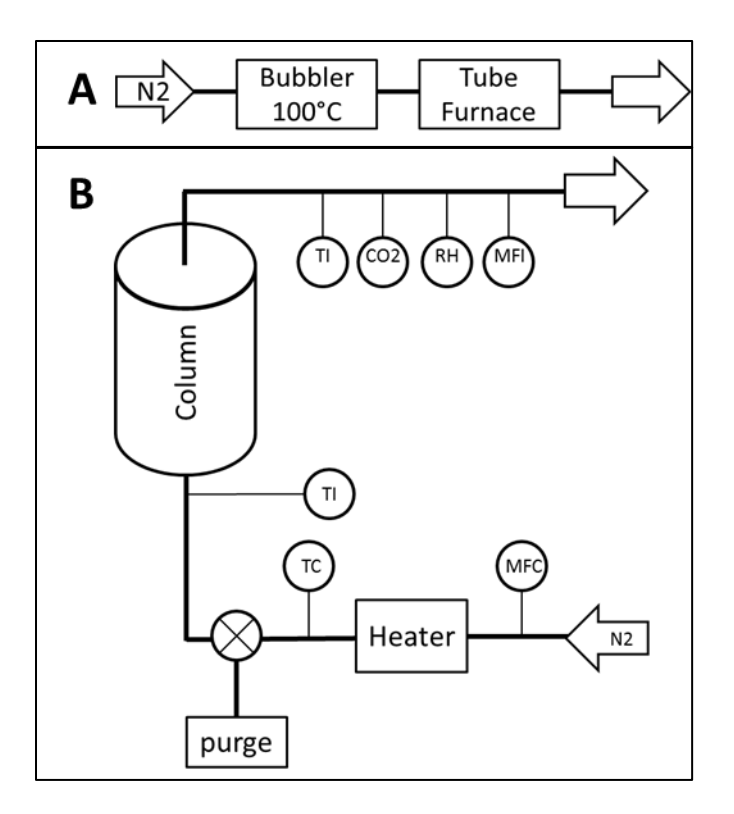


Figure 2: Process diagram of regeneration in a tube furnace (A), where CO₂ was stripped from all six MECS types during preliminary testing. (B) Process diagram of the regeneration apparatus used to strip CO₂ using a dry stream of N₂ at ~90°C during the 10-cycle experiments (MFC= mass flow controller, TC= temperature controller, TI= temperature indicator, CO2= CO₂ sensor, RH= relative humidity sensor, MFI= mass flow indicator).

For the 10-cycle tests, a lower temperature regeneration set-up was implemented to prevent MECS dehydration and mass loss. The MECS were stripped of CO_2 for one hour by using a stream of dry N_2 at ~90°C, as shown schematically in Figure 2B. The gas stream was heated to 300°C but the temperature at the bottom of the regeneration column was measured to be ~95°C (± 5 °C) due to heat loss along the tubing. Following regeneration, the sodium carbonate MECS were soaked overnight in a 17 wt% sodium carbonate solution to allow them to rehydrate. The carbonate MECS were then rinsed and dried with compressed air before testing in the pressure drop apparatus to maintain a relatively constant sample mass across cycles. The ionic liquid MECS were taken immediately from the regeneration apparatus, weighed, and then placed in the pressure drop apparatus. Images and masses of the MECS were recorded at each step of the cycling process. In these cycling tests, the MECS were enclosed within a fine mesh cartridge to minimize attrition during transfers.

3. Results and Discussion

3.1 Preliminary MECS screening

We used a temperature-controlled chamber in which CO₂ could be injected in the absence of other gases and the total pressure of the chamber monitored over time to measure the CO₂ absorption by the MECS. The drop of pressure following injection of CO₂, shown with representative data in SI, was attributed to the absorption of CO₂ into the MECS capsules and used to calculate the number of moles of CO₂ absorbed by the MECS as a function of time. From this data, the rate of CO₂ absorption and the stoichiometric capacity of the MECS can be calculated. As the rate of CO₂ absorption depends on both CO₂ partial pressure and the temperature, we first completed some preliminary experiments to verify our method.

First, experiments were performed on the uncatalyzed Na₂CO₃ capsules to determine if our experiment could be carried out at CO₂ partial pressures similar to that of flue gas from a coal-fired power plant, ~0.1 bar CO₂, and whether or not the presence of air affects the CO₂ absorption by the MECS. We have previously measured the permeability of the MECS shell materials to nitrogen and CO₂ separately, shown in Table 1, but had not investigated the effect of a mixed gas stream on the absorption rate of CO₂ by the MECS until now. The selectivity of a membrane between a pair of gases is given by

$$\alpha_{A/B} = \frac{P_A}{P_B} \tag{3}$$

in which P_A is the permeability of the more permeable gas and P_B is the permeability of the less permeable gas.²¹ In the case of the both types of silicone shells used in the MECS, the selectivity for CO_2 over N_2 is ~11, which is on the low end compared to other materials reported in literature.^{22,23} Additionally, previous research suggests that the presence of nitrogen can reduce CO_2 permeability in silicones that have similar molecular structure to the MECS shell materials²⁴, which would be detrimental to the rate of CO_2 absorption from coal flue gas in which nitrogen makes up ~75% of the gas stream. The CO_2 permeability of the silicone shell must remain high in the presence of CO_2 mixed with air to avoid the absorption rate being limited by mass transfer of CO_2 to the solvent. In order to test whether the CO_2 absorption rate was affected by the presence of air, CO_2 absorption tests were performed in the pressure drop chamber with 0.1 bar of injected CO_2 in both cases and an additional 0.9 bar of ambient atmosphere (79% N_2) injected in the case with air. The resulting total molar fluxes for these two cases are compared in Figure 3 over the first 10 minutes, the region of the loading curve where CO_2 diffusion through the shell material is typically rate-limiting. Permeability is related to molar flux, J, by

$$P = \frac{J^*d}{\Delta p} \tag{4}$$

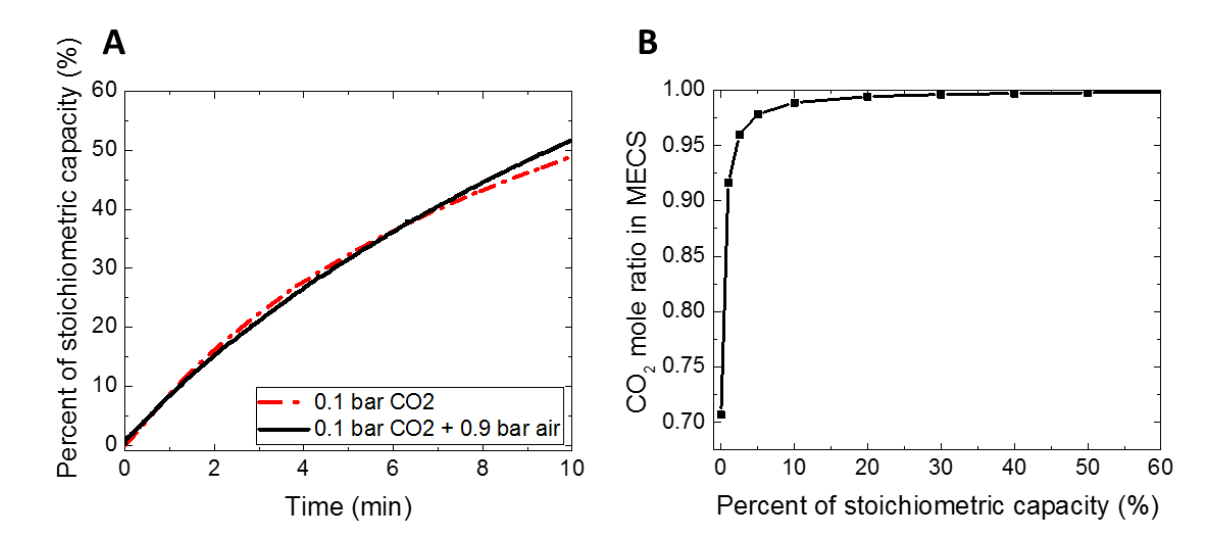
where d is the thickness of the membrane, or in this case the shell thickness, and Δp is the pressure difference across the membrane. Combining Eq. 4 with Eq. 3 and assuming that the selectively for CO_2/N_2 remains ~11, the ratio of fluxes is proportional to the partial pressure gradient across the shell, given by Eq. 5

$$\frac{J_{CO2}}{J_{N2}} = \alpha_{A/B} \frac{\Delta p_{CO2}}{\Delta p_{N2}}$$

Assuming the total molar flux $J = J_{CO2} + J_{N2}$ we expect to see ~1.6 times the total flux in the presence of air compared to CO_2 alone if J_{CO2} remains the same in both cases. However, we observed that the slope of the loading curves (proportional to the flux) was nearly the same in both cases, as shown in Figure 3A.

We used a model incorporating the gas solubilities in both the shell and core solution and the gas permeabilities in silicone to estimate the mole ratio of CO_2 in the MECS (shell and core) as a function of CO_2 loading in the core solution. Due to the consumption of CO_2 by reaction with carbonate inside the capsules and the resulting increase in bicarbonate concentration, the solubility of CO_2 in the MECS core is always at least an order of magnitude greater than that of N_2 . In Figure 3B, the model was used to calculate that the mole ratio of CO_2 in the MECS should jump quickly from ~70% for unloaded capsules to ~91% in capsules that have reached 5% loading capacity in 0.1 bar CO_2 and 0.9 bar N_2 conditions; this loading is achieved in less than a minute. The model indicates that CO_2 solubility will be so high that in this shell-limited regime $\Delta p_{CO2} >> \Delta p_{N2}$ as the capsules equilibrate with N_2 and Δp_{N2} goes to zero. This means the N_2 contribution to the loading and molar flux becomes negligible relative to CO_2 in less than a minute. Since the loading curves in Figure 3A are nearly the same, we can conclude that the N_2 absorption is negligible (<0.2 mole% at 10 minutes) and that the presence of air has no significant impact on the CO_2 absorption by MECS.

Since N_2 has a negligible impact on the CO_2 absorption into the MECS, we simplified our experiments by filling the pressure drop chamber with only ~0.1 bar of CO_2 (not adding N_2 or air as the balance), which allows the pressure drop signal to be interpreted as solely due to CO_2 absorption by the MECS. Based on the model and experimental results, we do not expect the CO_2 absorption rate of MECS in clean flue gas containing a low partial pressure CO_2 mixed with nitrogen to be significantly different. However, we did not investigate the effect of water vapor concentration on CO_2 absorption by MECS, and flue gas can contain up to about 5% water vapor.



227

228

229

230

231

232

233

234

235236

237

238

239

240241

242

243

244

245

246

247

248

249

250

251

252

253

Figure 3: A) Loading capacity versus time for uncatalyzed Na₂CO₃ MECS exposed to 0.1 bar CO₂ with and without 0.9 bar air in the pressure drop apparatus at 25°C. The loading was practically the same in pure CO₂ as in CO₂ with air. B) Model calculation of CO₂ mole ratio of CO₂ and N₂ in MECS (shell and core) in 0.1 bar CO₂ and 0.9 bar N₂ condition as a function of CO₂ loading capacity. The ratio quickly approaches 100%, meaning N₂ contribution to the flux and loading may be assumed to be negligible.

As described in an earlier publication, we have devised methods for encapsulating diverse solvent types including CO₂BOLs and ionic liquids in CO₂-permeable polymer shells. ¹⁶ Table 1 displays the composition and properties of each of the six MECS types tested in this report: 1) uncatalyzed Na₂CO₃ MECS, 2) Na₂CO₃ MECS with 50 mM cyclen, 3) Na₂CO₃ MECS with 600 mM sarcosine, 4) NDIL0309 MECS, 5) NDIL0230 MECS, and 6) CO2BOL MECS. Na2CO3 was chosen as a solvent due to its ease of handling and environmental compatibility, but since it suffers from low rate of reaction we chose to also study the effect of two different promoters. Here we used a 17 wt% solution of Na₂CO₃ in the MECS because that is the highest soluble concentration at room temperature; for a post-combustion process we would like to use 30-40 wt% Na₂CO₃ MECS with greater CO₂ absorption capacity by preparing the MECS in a heated device to increase the carbonate solubility. The ionic liquids and CO₂BOL offer increased rate of CO₂ absorption and loading capacity but present challenges in the form of high viscosity, phase changes, and potential environmental toxicity, which encapsulation may surmount. The solvent volume fraction of each capsule type, shown in Table 1, was calculated based on the ratio of volumetric flow rates of core and shell during the microencapsulation process, and for the ionic liquid and CO₂BOLcapsules it is calculated on a dry basis. Consequently, the solvent volume fraction is lower for the ionic liquid and CO₂BOL MECS because they were prepared in solution with water to reduce the solvent viscosity, and then the water was dried out by lyophilization following fabrication. The average MECS capsule diameter is a function of flow rates and viscosities of the three emulsion fluids, and thus varies across the different solvent types. However, the variation in volume fractions and diameters is small enough not to confound absorption comparisons. The shell material was

different for the IL MECS to overcome solvent-shell compatibility issues that hindered their fabrication. For all MECS types the shell thickness is on the order of tens of microns and all shell materials used uptake CO_2 on the order of $1x10^{-5}$ moles of CO_2 per gram of silicone, which is at least three orders of magnitude less than that of MECS and thus negligible.

Table 1: Comparison of the six candidate sorbent capsule compositions and properties¹.

Solvent Type	Solvent Description	Solvent Volume Fraction	Average Diameter (µm)	MECS Shell Material	Shell Thickness (µm)	CO ₂ permeability (Barrer)	N ₂ permeability (Barrer)
17 wt% Na ₂ CO ₃ Solution	no catalyst	0.67	300 ± 8	Tegorad 2650	20	3250	280
	50 mM cyclen	0.67	370 ± 20	Tegorad 2650	20	3250	280
	600 mM sarcosine	0.67	320 ± 6	Tegorad 2650	20	3250	280
Ionic	NDIL0309	0.51	390 ± 6	Thiolene-Q	30	2680	250
Liquid	NDIL0230	0.33	422 ± 27	Thiolene-Q	40	2680	250
CO ₂ BOL	Koechanol	0.40	508 ± 38	Tegorad 2650	40	3250	280

¹The three rows in bold correspond to the MECS that underwent 10-cycle tests.

In this report, we evaluate CO₂ loading rates, stoichiometric capacities, and MECS stability over absorption/regeneration cycling of these six solvents for the first time. As a preliminary test to evaluate the feasibility of regenerating the MECS in a heated nitrogen environment, we completed 3 cycles in the CO₂ pressure drop setup (absorption) and regeneration in a tube furnace with N₂ flow at 130°C (stripping) for each of the six MECS formulations in Table 1, and compared the change in mass of the MECS and CO₂ absorption versus time from cycle to cycle to determinate the success of regeneration and stability of the MECS.

The Koechanol CO₂BOL MECS lost 33% of their mass on average each time they were regenerated in the tube furnace, as shown in Figure 4. Microscope images of Koechanol MECS taken after regeneration confirm that Koechanol leaks through the capsule shell. The visible droplet formation, collapsed capsules, and declining mass observed in Figure 4 indicate that Koechanol did not remain encapsulated while cycling. We hypothesize that because CO₂BOLs are small, nonpolar molecules when they are not bound to CO₂ perhaps they are able to diffuse across the silicone shell of the MECS. Though the MECS were not visibly cracked or broken in the microscope images, it is also possible that some reaction between the Koechanol and the silicone shell resulted in incomplete curing of the shell or formation of microcracks in the shell that are exacerbated by regeneration at increased temperature. While we have not yet confirmed the mechanism of Koechanol leaking, because the mass loss over absorption/regeneration cycling is undesirable the Koechanol CO₂BOL was ruled out from further tests.

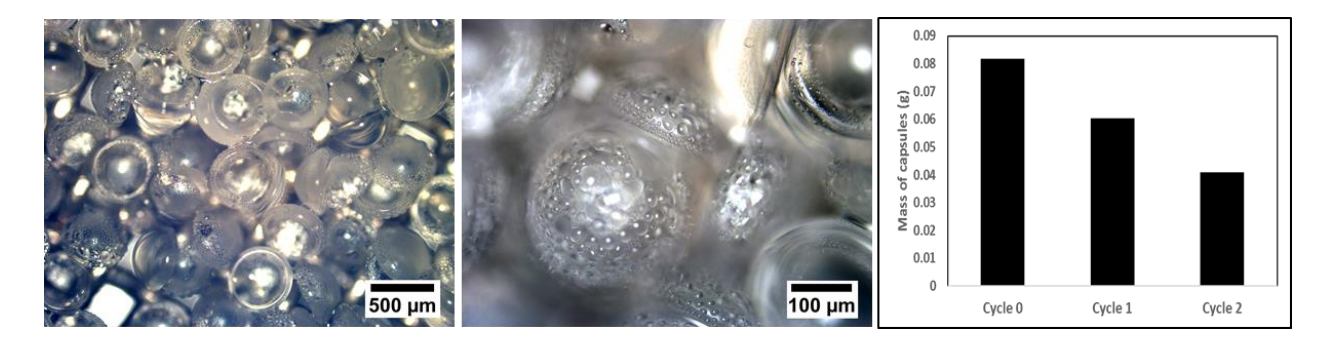


Figure 4: Microscope images of Koechanol CO₂BOL MECS after exposure to desiccant for 4 days before cycling, with visible droplets on the shell surface. The mass of Koechanol MECS decreases dramatically with each absorption/regeneration cycle (right).

Next, we compared the Cycle 0 loading curves for the three Na₂CO₃ MECS types at 25°C to determine whether the addition of the promoters cyclen or sarcosine affects the CO₂ absorption rate compared to uncatalyzed Na₂CO₃ MECS. As shown in Figure 5A, we found that the addition of promoters has the greatest effect on CO₂ loading rate during the first 5 minutes of loading. Although sarcosine has the highest CO₂ reaction rate among common amino acids, it is well known that the reaction rate of amino acids is strongly dependent on solution pH, and thus the effect of sarcosine may be limited by its relatively high pKa of 10.2. 18,25 Figure 5A shows that the absorption rate of Na₂CO₃ MECS with sarcosine was initially at least twice that of Na₂CO₃ MECS with cyclen, but decreased rapidly within the first two minutes of loading as the pH of the solution inside the capsules decreased below the pKa of sarcosine; at 10 minutes, the CO₂ absorption rate was no longer enhanced by the amino acid relative to uncatalyzed Na₂CO₃ MECS. This is comparable to what others have reported; Hu et al. observed a 6x increase in CO₂ absorption rate of 500 mM sarcosine in 30 wt% potassium carbonate at pH 12.5 but no rate enhancement by sarcosine at a neutral pH.²⁵ As the pH of our solution was only ~11.2 and we ran our experiment at 25°C rather than 50°C, we would expect the initial rate increase of our solution to be less than 6x, so our measured value of 2x appears consistent.

The cyclen promoter, on the other hand, increased the CO_2 loading rate compared to uncatalyzed MECS over 20 minutes of the loading curve in Figure 5A, as the pKa of cyclen is ~7.9¹⁹, with the largest increase again occurring in the first 5 minutes of the loading curve Previous studies with MECS containing a 3 wt% potassium carbonate solution and cyclen indicated an instantaneous absorption rate increase of twice as much as that of uncatalyzed potassium carbonate¹⁵; however, with a more concentrated 17 wt% sodium carbonate solution here we find an initial ~1.5x rate increase with cyclen compared to uncatalyzed sodium carbonate MECS. This could be due to product inhibition between the carbonate and zinc (II) cyclen at high pH.²⁰

These results emphasize the importance of determining which parameters will guide process design; at loading times up to 5 minutes promotors such as sarcosine or cyclen will improve reaction kinetics but the MECS achieve less than 50% of their loading capacity in that time, shown in Figure 5B. However, at loading times much greater than 5 minutes the kinetic benefit of adding

a promotor becomes negligible but all three sodium carbonate MECS reach higher working capacity on a per-mass basis. Both absorption rate and loading capacity are important parameters for sizing the absorption vessel and determining economic feasibility of the system, so an optimum working capacity likely exists to take advantage of higher rates early in the loading curve but still reach high enough loading capacity to require a reasonably sized absorber.

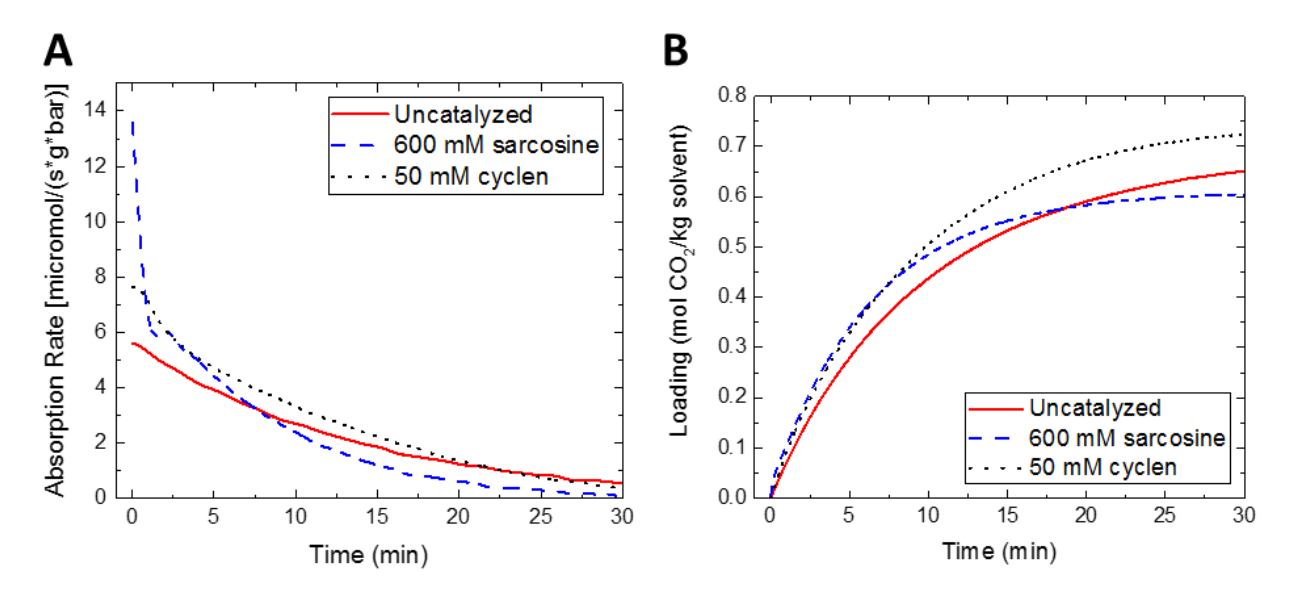


Figure 5: Comparison of CO₂ absorption vs time for the three types of Na₂CO₃ MECS: uncatalyzed MECS, MECS with sarcosine promoter, and MECS with cyclen promoter. All of these MECS contained 17 wt% Na₂CO₃ and were soaked in 17 wt% Na₂CO₃ solution prior to testing. All data were collected in the pressure drop at room temperature (25°C). A) CO₂ absorption rate normalized by MECS mass and initial pressure, B) CO₂ loading normalized by MECS mass.

The loading trends shown in Figure 5 were repeatable over the preliminary 3 absorption/stripping cycles for the three Na_2CO_3 MECS types. It is likely that the effect of the cyclen catalyst would be more pronounced at temperatures greater than $25^{\circ}C$, as the activity of cyclen is known to increase dramatically from $25^{\circ}C$ to $75^{\circ}C$. Based on preliminary cycling results and the potential for kinetic improvement across the entire loading curve, Na_2CO_3 -cyclen was selected from the three carbonate MECS types for further testing at various temperatures to see if higher temperatures would increase the effect of the promoter cyclen and to confirm that the cyclen remains stable though repeated regeneration at temperatures up to $100^{\circ}C$.

The NDIL0230 and NDIL0309 ionic liquid MECS performed consistently across the preliminary three absorption/regeneration cycles without any mass loss (data in SI). Therefore, both of the ionic liquid MECS were selected for additional evaluation alongside the Na₂CO₃-cyclen MECS.

CO₂ absorption rates and CO₂ capacities are temperature-dependent, so the CO₂ absorption of the Na₂CO₃-cyclen, NDIL0309, and NDIL0230 MECS was tested over several temperatures. While both the reaction rate of CO₂ with solvents and the permeability of silicone increase with temperature^{22,26}, the solubility of CO₂(aq) and the equilibrium CO₂ capacity of solvents tend to decrease with temperature. Figure 6A shows that as expected, higher temperatures increase the rate of CO₂ absorption by Na₂CO₃ MECS, but only for the first couple minutes of the loading curve.

342

343

344

345346

347

348

349

350

351

352

353

354

355

356

357358

359

360

361

362

363

364

365

366367

368

369

370371

372

As noted in a publication by Seo et al., the phase change ionic liquid NDIL0309 should remain in the solid phase at temperatures below 60°C upon exposure to dry CO₂ and thus all absorption of CO₂ at temperatures below this temperature should be primarily limited by mass transfer to surface adsorption. ¹⁴ However, we observed that upon typical handling in ambient atmospheric conditions at room temperature, NDIL0309 changed from solid phase to liquid phase within minutes regardless of whether it was encapsulated in MECS due to the deliquescent nature of NDIL0309, as shown previously by Seo et al. Images of the liquid core of NDIL0309 MECS exposed to atmospheric conditions are shown in Figure 9. We measured the mass increase due to this water uptake to be 2-3 wt% of the ionic liquid at room temperature, but it should be noted that the physical mechanism of this phase change and its effect on CO₂ uptake is not understood and direct comparisons to pure, dry NDIL0309 at temperatures below 60°C cannot be drawn. We feel that our CO₂ absorption data collected at 25°C and 40°C are relevant to report because of the ubiquitous presence of water vapor in flue gas capture, increasing the likelihood that NDIL0309 will be in the liquid phase and able to absorb CO₂ at lower temperatures but eliminating the advantage of the phase change from solid to liquid upon CO₂ uptake. Figure 6B shows that temperature has insignificant effect on CO2 absorption rate by NDIL0309 MECS, and Figure 6C shows that only 60°C increases the CO₂ absorption rate in NDIL0230 MECS.

Figure 6D shows that after 30 minutes of absorption, the net effect is a decrease in absorbed CO₂ with increasing temperature for all three MECS, due to the decreased solubility in the solvents at higher temperature. At 25°C, the Na₂CO₃ MECS reached 45% stoichiometric CO₂ capacity, while NDIL0230 and NDIL0309 MECS reached 53% and 65% of their stoichiometric capacities, respectively. At 60°C the stoichiometric capacities of the Na₂CO, NDIL0230, and NDIL0309 MECS were 17%, 39%, and 51%, respectively. Despite the increased activity of cyclen at higher temperature, shown by a higher absorption rate in the first two minutes, the decreased solubility of CO₂ in Na₂CO₃ MECS at higher temperatures results in decreased CO₂ capacity with temperature. Despite the water content, the ionic liquid MECS capacities are similar to previous results from CO₂ absorption experiments run with pure ionic liquids at low partial pressures of CO₂; Seo et al. reported 68% stoichiometric capacity of NDIL0309 at 60°C¹⁴ and 78% stoichiometric capacity for an IL similar to NDIL0230 at 22°C.¹¹ The CO₂ capacity data from Seo et al. were based on isotherm experiments in which CO₂ absorption was measured at equilibrium after several hours, whereas our CO₂ working capacity data is based on CO₂ absorption over 30

minutes and thus our lower loading may reflect diffusion limitations as well as complications from the water uptake.

Based on the results of CO₂ absorption at various temperatures, the 10-cycle absorption tests were all performed at 25°C to maximize the CO₂ loading capacity. Running the experiments at room temperature also enabled more accurate and reproducible temperature and humidity control.

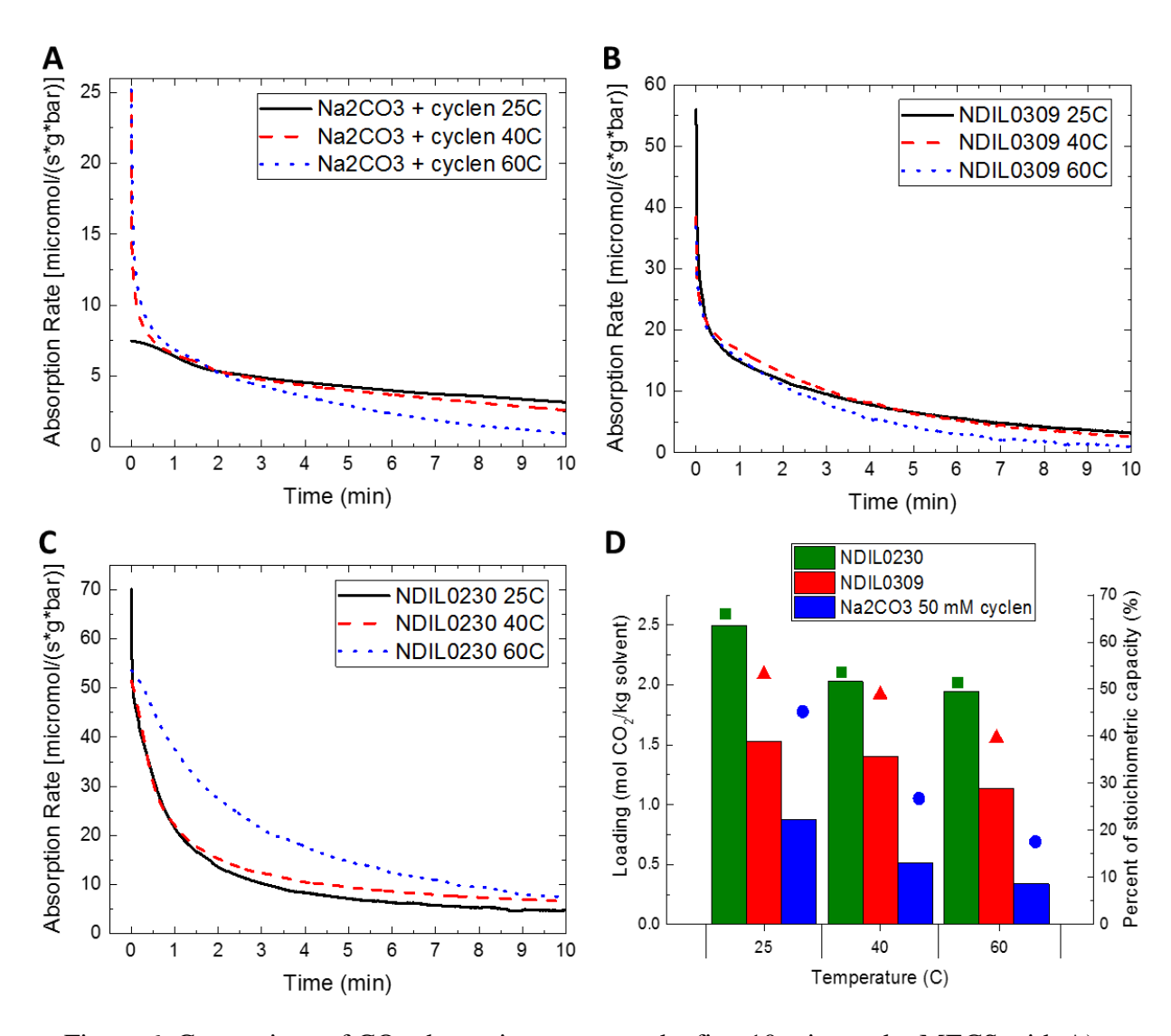


Figure 6: Comparison of CO₂ absorption rate over the first 10 minutes by MECS with A) Na₂CO₃-cyclen, B) NDIL0309, and C) NDIL0230, and at 25, 40, and 60°C. D) The bar graph displays CO₂ loading after 30 minutes (left axis), and the markers represent the percent of stoichiometric capacity (right axis) of each solvent.

Each of the three final candidate MECS (Na₂CO₃-cyclen, NDIL0309, NDIL0230) was subjected to 10 absorption/regeneration cycles, as detailed in the Methods section. The initial (Cycle 0) CO₂ loading of the three MECS is compared in Figure 7A. We present the CO₂ working loading

capacity at 30 minutes as this is the amount of time it takes for the curve to approach an asymptote, although it is worth noting that the amount of time for the MECS loading to reach true equilibrium capacity would be on the order of hours. In order to fairly compare the CO₂ absorption of the three solvent types, we normalized the moles of CO₂ absorbed by the mass of the solvent since the solvent is the reactive portion of the MECS and we were primarily interested in comparing absorption as a function of time and stoichiometric capacity. For other applications such as CO₂ transportation, storage, or absorber sizing it may make more sense to normalize by the total mass or volume of MECS. As the loading is normalized by the total solvent mass, the ionic liquids reach higher values because they contain no water, while the sodium carbonate solution is comprised of 83% water.

Figure 7B displays capacities as a percentage of total CO₂ stoichiometric capacity of each solvent. In terms of stoichiometric capacity, all three MECS types reach at least 40% capacity within 30 minutes. None of the MECS exceed ~60% stoichiometric capacity, and this is because stoichiometric capacity is affected by the partial pressure of CO₂; at CO₂ partial pressure of 0.1 bar we expect stoichiometric capacities in the range of 10-80% whereas at 1 bar of CO₂ the uptake can approach 100%, depending on the IL and temperature. Additionally, since the experiment is carried out in a batch-type process, the loading equilibrates to a CO₂ partial pressure much less than 0.1 bar; a typical final CO₂ partial pressure is ~0.05 bar. In an actual process, adsorption would be conducted in a flow-through column to provide a constant CO₂ partial pressure of 0.1 bar at the column inlet.

Both ionic liquid MECS types have an initial loading rate that is much higher than that of sodium carbonate MECS. Over the course of 30 minutes, however, the stoichiometric loading capacity of the carbonate MECS matches that of NDIL0309. This again highlights that the parameters chosen for comparison depend on the constraints for process design; if it is practical to load MECS for a period as short as 10 minutes, then the kinetics of the ionic liquid MECS make them advantageous to sodium carbonate MECS. However, if longer loading periods are practical then the kinetics of the absorption are less of a factor and the carbonate MECS perform comparably to ionic liquids in terms of stoichiometric capacity. The NDIL0230 ionic liquid capsules outperform both other MECS types in stoichiometric CO₂ loading capacity by about 20%. If the CO₂ loading on a permass basis is an important parameter for consideration then the IL MECS vastly outperform the Na₂CO₃ MECS because they do not have additional water mass. However, in industrial operation, the Na₂CO₃ MECS will likely be prepared at higher concentrations and thus have higher capacities.

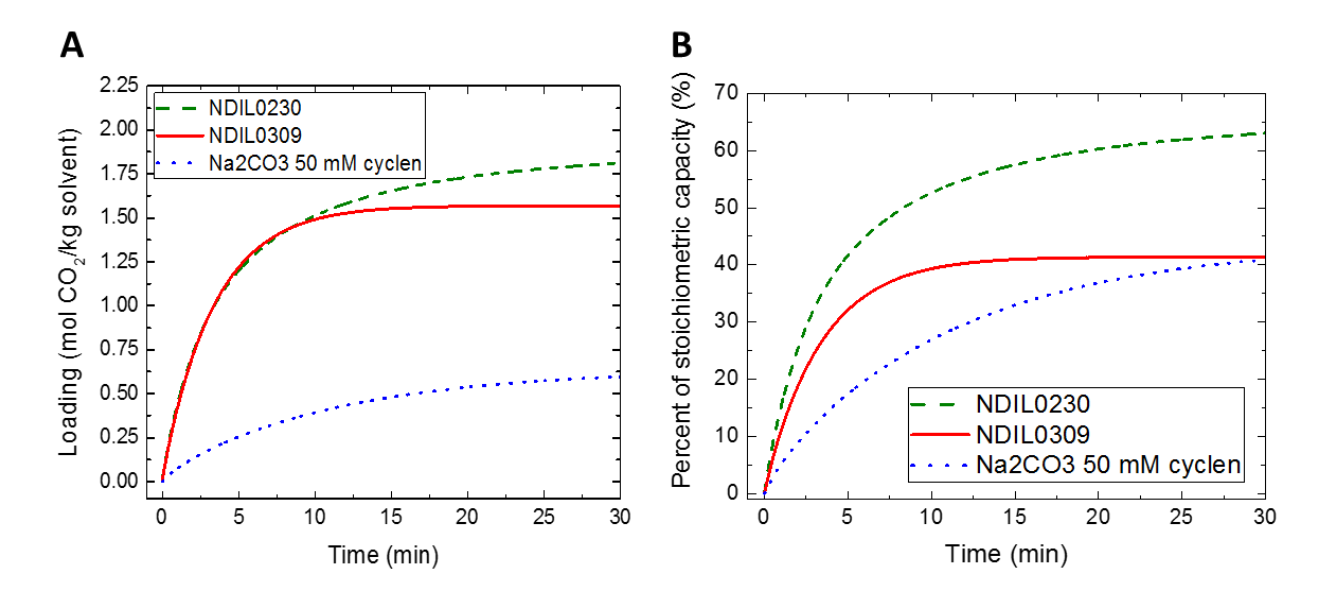


Figure 7: Comparison of CO₂ loading vs. time for three MECS (NDIL0230, NDIL0309 and Na₂CO₃-cyclen) during Cycle 0 at 25°C and 0.1 bar CO₂. CO₂ loading is presented in terms of mol/kg solvent (left) and as a percentage of total stoichiometric capacity (right).

420

421

422

423

424

425

426

427 428

429

430

431

432

433

434

435

436 437

438

The CO₂ absorption results for the three MECS types are compared across the 10 cycles in Figure 8A in terms of moles CO₂/kg solvent and percent of total stoichiometric capacity in Figure 8B (lines). The CO₂ absorption for ionic liquid NDIL0230 MECS is remarkably reproducible across the 10 cycles (average across 10 cycles of 1.610 mol/kg solvent, standard deviation 0.075) and consistently reaches ~10% higher stoichiometric capacity than the other two MECS types. Though there is more variation in the CO₂ absorption by NDIL0309 MECS (average across 10 cycles of 1.607 mol/kg solvent, standard deviation 0.137) and Na₂CO₃-cyclen MECS (average across 10 cycles of 0.665 mol/kg solvent, standard deviation 0.083) across ten cycles, the capacity is fairly consistent and shows no downward trend, which would indicate degradation of the solvent or cyclen. These cycling results confirm that performance does not degrade over cycling with heat regeneration and that CO₂ is being effectively stripped from all three MECS types using a relatively low-temperature regeneration process. This is especially important in the case of the Na₂CO₃-cyclen MECS, as there was concern of degradation of the cyclen catalyst at higher carbonate concentration and elevated temperature. ²⁰ The regeneration temperature of ~90-100°C is on the low end of the typical range of 100-140°C and thus could provide a reduction in the energy cost of regeneration.²⁹

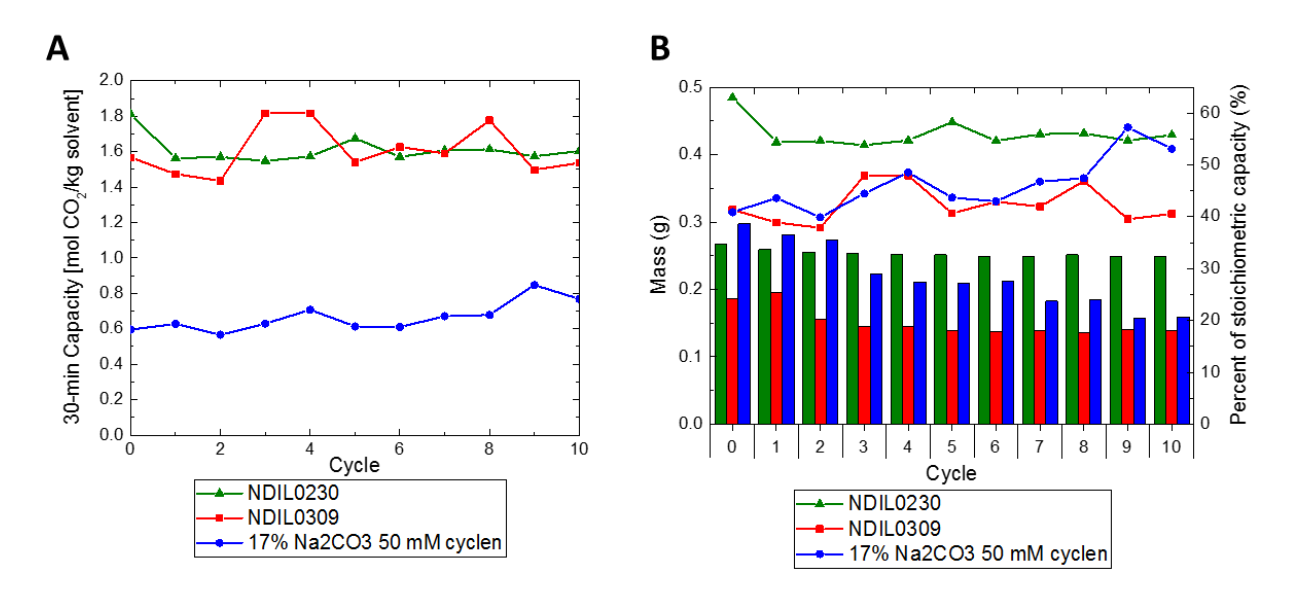


Figure 8: Comparison of CO₂ absorbed by three MECS types (NDIL0230, NDIL0309 and Na₂CO₃ w/cyclen) across 10 cycles. CO₂ loading capacities are the cumulative CO₂ absorbed (per kg solvent and initial pressure) after the MECS have been exposed to CO₂ in the pressure drop apparatus for 30 minutes. A) CO₂ loading is presented in terms of mol/kg. B) The mass of the MECS is shown over 10 cycles (bars, left axis) and CO₂ loading is shown as a percentage of total stoichiometric capacity (lines, right axis).

440

441

442443

444

445

446

447

448

449

450

451

452

453

454

455

456

457

458

459

460

461

462

463

464

465 466 We report the mass of the MECS, measured immediately before putting the MECS in the pressure drop to absorb CO₂ for each cycle, in Figure 8B (bars) since in the preliminary studies with all 6 candidate solvents mass loss was indicative of the solvent leaking or perhaps the capsules breaking. Ionic liquid NDIL0230 MECS have a remarkably consistent mass across all cycles, indicating that the MECS aren't absorbing/desorbing ambient water vapor during handling, losing solvent through the shell, or breaking/degrading. Ionic liquid NDIL0309 MECS also have a reasonably consistent mass after the first few cycles. The mass loss after the first two cycles may be attributed to incomplete drying of the water from the capsules during lyophilization, absorption of water during storage and handling, or breaking of some MECS. The mass of the Na₂CO₃ MECS, in comparison, decreases steadily across the 10 cycles. This trend is a result of capsule attrition during the soaking step that follows regeneration, which involves transferring and recovering MECS to and from Na₂CO₃ solution for each cycle. We found that rehydration of sodium carbonate MECS following regeneration was critical to their ability to absorb CO₂, but it presents a challenge for repeatable measurements. In industrial operation, the capsules would be exposed to wet flue gas during absorption and steam during regeneration, likely being less prone to drying and reaching a steady state water balance over multiple cycles.

Figure 9 compares bright field microscopy images of the three MECS types before and after the 10 absorption/desorption cycles. It can be seen in the images that all MECS appear to remain intact following the cycling and change very little in diameter or shape. The homogeneity in size and geometry with cycling is helpful for absorber/stripper design, as volumetric or geometric changes would significantly affect vessel sizing, fluidization, and material handling of the MECS.

However, in comparing Figures 9C and 9F, it appears that the NDIL0230 MECS become discolored and textured after cycling, which could indicate a reaction between the ionic liquid and the polymer shell. Further shell compatibility tests should be performed on this ionic liquid to determine if degradation from solvent/shell reactions is an issue for long-term performance. Mechanical properties, water sensitivity, and CO₂ selectivity of the MECS, are also important for fluidized bed absorber operation for post-combustion CO₂ capture.

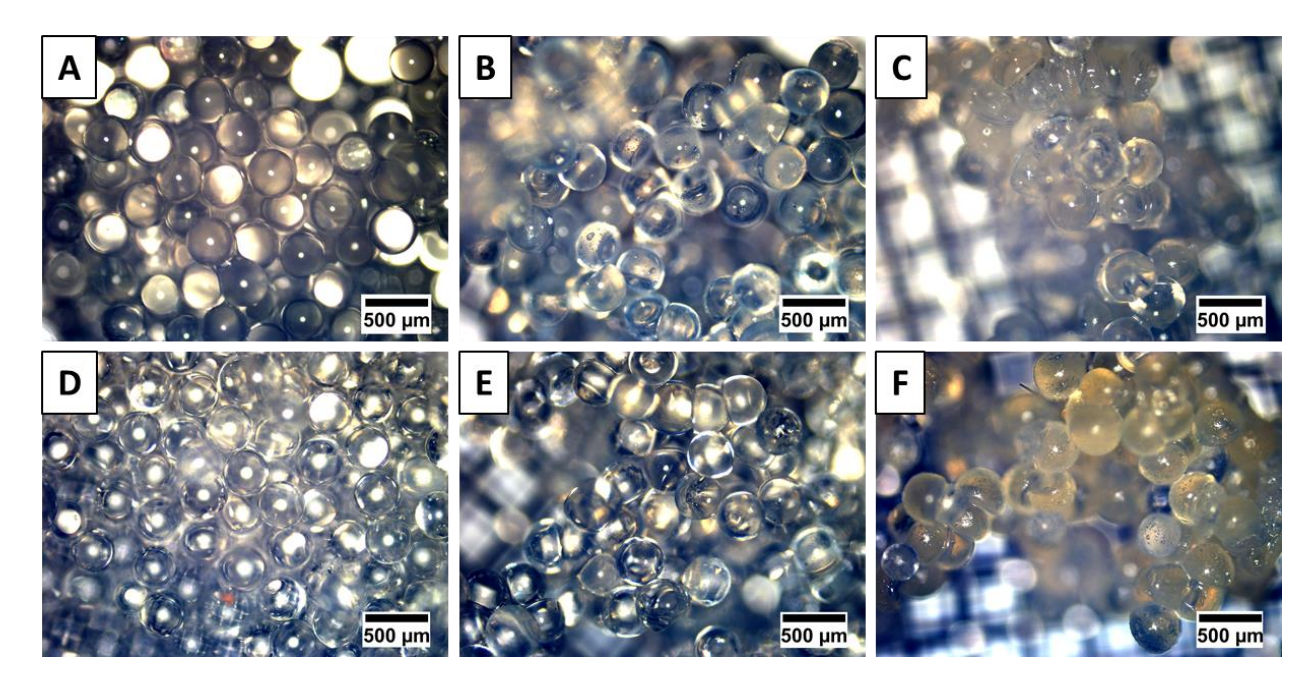


Figure 9: Microscope images of the three final candidate capsules taken before (top) and after (bottom) ten absorption/desorption cycles: A) Na₂CO₃ before cycling; B) NDIL0309 before cycling; C) NDIL0230 before cycling; D) Na₂CO₃ after ten cycles; E) NDIL0309 after ten cycles; F) NDIL0230 after ten cycles. The scale bar for each image is 500 μm.

Of three types of sodium carbonate MECS, the type promoted by cyclen catalyst performed the best, reaching a higher loading at a faster rate than one promoted by sarcosine or sodium carbonate solution alone. However, the performance enhancement was slight compared to the 2-times rate enhancement previously reported for potassium carbonate capsules. Among three water-lean solvents tested, the MECS filled with the CO₂-binding organic liquid Koechanol did not survive repeated cycles, apparently due to solvent escaping the capsule shells. The two ionic liquids, however, appear viable, with both NDIL0309 and NDIL0230 showing faster absorption rates and higher loading capacity than sodium carbonate capsules and remarkable stability over 10 regeneration cycles. Of all types studied, NDIL0230 MECS performed the best.

The two IL MECS had cyclic loadings that compare favorably to aqueous amines. At 25°C and 0.05—0.1 bar of CO₂, NDIL0230 loaded 2.5 moles CO₂/kg solvent and NDIL0309 loaded 1.5 moles CO₂/kg solvent. Na₂CO₃-cyclen loaded 0.8 moles CO₂/kg solvent, but this is expected to be higher when MECS are produced with more concentrated core solution, as discussed above. A typical cyclic capacity for aqueous monoethanolamine is 1.5 moles CO₂/kg solvent.⁷

- 492 At the tested partial pressures, the measured working capacities also compare favorably with many
- solid sorbents for CO₂ adsorption such as activated carbons (0.5-0.75 moles CO₂/kg sorbent),
- zeolites (0.5-2.6 moles CO₂/kg sorbent), and alkali carbonates on solid supports (0.5-2.9 moles
- 495 CO₂/kg sorbent). The relative mass of the shell material to the encapsulated solvent can be reduced
- by refining fabrication methods, but the capacities of MECS will be lower per unit of total sorbent
- 497 mass than per unit of solvent.
- 498 Overall, across the characteristics tested here absorption rate, capacity, and cyclic stability the
- 499 ionic liquid MECS appear to be a potential competitor to aqueous amines. The major challenge to
- these MECS are common to solid sorbents: the need for a process configuration that is similar in
- capital cost and energy efficiency to aqueous solvent systems. Further work is needed on material
- fabrication and testing at larger scale to establish the viability of IL MECS.
- 503 <u>Acknowledgements</u>
- This work was performed under the auspices of the U.S. Department of Energy by Lawrence
- Livermore National Laboratory under Contract DE-AC52-07NA27344. Funding was provided by
- the U.S. Department of Energy, Office of Fossil Energy under awards DE-FE0026465 and FEW-
- 507 0194. Release number LLNL-JRNL-746767.
- 508 References
- 509 1. Center for Climate and Energy Solutions. Global Emissions. Available at:
- 510 https://www.c2es.org/content/international-emissions/.
- 2. Le Quéré, C. et al. Global Carbon Budget 2016. Earth Syst. Sci. Data 8, 605–649 (2016).
- 3. Lewis, N. S. Aspects of science and technology in support of legal and policy frameworks
- associated with a global carbon emissions-control regime. *Energy Env. Sci* **9,** 2172–2176
- 514 (2016).
- 515 4. Pachauri, R. K. & Meyer, L. A. IPCC, 2014: Climate Change 2014: Synthesis Report.
- Contribution of Working Groups I, II and III to the Fifth Assessment Report of the
- 517 Intergovernmental Panel on Climate Change. 151 (IPCC).
- 5. U.S. Energy Information Administration. How much of U.S. carbon dioxide emissions are
- sociated with electricity generation? Available at:
- 520 https://www.eia.gov/tools/faqs/faq.php?id=77&t=11.

- 521 6. Rochelle, G. T. Amine scrubbing for CO2 capture. *Science* **325**, 1652–1654 (2009).
- 522 7. Samanta, A., Zhao, A., Shimizu, G. K. H., Sarkar, P. & Gupta, R. Post-Combustion CO2
- 523 Capture Using Solid Sorbents: A Review. *Ind. Eng. Chem. Res.* **51,** 1438–1463 (2012).
- 8. Heldebrant, D. J., Yonker, C. R., Jessop, P. G. & Phan, L. Organic liquid CO2 capture agents
- with high gravimetric CO2 capacity. *Energy Environ. Sci.* **1,** 487–493 (2008).
- 526 9. Zhang, J. et al. CO2-Binding-Organic-Liquids-Enhanced CO2 Capture using Polarity-Swing-
- Assisted Regeneration. *Energy Procedia* **37**, 285–291 (2013).
- 528 10. Brennecke, J. F. & Gurkan, B. E. Ionic Liquids for CO2 Capture and Emission Reduction. J.
- 529 *Phys. Chem. Lett.* **1,** 3459–3464 (2010).
- 530 11. Seo, S., DeSilva, M. A., Xia, H. & Brennecke, J. F. Effect of Cation on Physical Properties
- and CO2 Solubility for Phosphonium-Based Ionic Liquids with 2-Cyanopyrrolide Anions. J.
- 532 *Phys. Chem. B* **119**, 11807–11814 (2015).
- 533 12. Seo, S. et al. Chemically Tunable Ionic Liquids with Aprotic Heterocyclic Anion (AHA) for
- 534 CO2 Capture. J. Phys. Chem. B 118, 5740–5751 (2014).
- 535 13. Sun, L., Morales-Collazo, O., Xia, H. & Brennecke, J. F. Effect of Structure on Transport
- Properties (Viscosity, Ionic Conductivity, and Self-Diffusion Coefficient) of Aprotic
- Heterocyclic Anion (AHA) Room Temperature Ionic Liquids. 2. Variation of Alkyl Chain
- 538 Length in the Phosphonium Cation. *J. Phys. Chem. B* **120**, 5767–5776 (2016).
- 539 14. Seo, S. et al. Phase-Change Ionic Liquids for Postcombustion CO2 Capture. Energy Fuels 28,
- 540 5968–5977 (2014).
- 541 15. Vericella, J. J. et al. Encapsulated liquid sorbents for carbon dioxide capture. Nat. Commun.
- **6,** 6124 (2015).

- 543 16. Stolaroff, J. K. et al. Microencapsulation of advanced solvents for carbon capture. Faraday
- 544 *Discuss* **192,** 271–281 (2016).
- 545 17. Zhang, S., Zhang, Z., Lu, Y., Rostam-Abadi, M. & Jones, A. Activity and stability of
- immobilized carbonic anhydrase for promoting CO2 absorption into a carbonate solution for
- 547 post-combustion CO2 capture. *Bioresour. Technol.* **102,** 10194–10201 (2011).
- 548 18. Thee, H. et al. A kinetic study of CO2 capture with potassium carbonate solutions promoted
- with various amino acids: Glycine, sarcosine and proline. *Int. J. Greenh. Gas Control* **20**, 212–
- 550 222 (2014).
- 551 19. Zhang, X. & van Eldik, R. A functional model for carbonic anhydrase: thermodynamic and
- kinetic study of a tetraazacyclododecane complex of zinc(II). *Inorg. Chem.* **34,** 5606–5614
- 553 (1995).
- 554 20. Floyd, W. C. *et al.* Evaluation of a Carbonic Anhydrase Mimic for Industrial Carbon Capture.
- 555 Environ. Sci. Technol. 47, 10049–10055 (2013).
- 556 21. Freeman, B. D. Basis of Permeability/Selectivity Tradeoff Relations in Polymeric Gas
- Separation Membranes. *Macromolecules* **32**, 375–380 (1999).
- 558 22. Powell, C. E. & Qiao, G. G. Polymeric CO2/N2 gas separation membranes for the capture of
- carbon dioxide from power plant flue gases. J. Membr. Sci. 279, 1–49 (2006).
- 560 23. Zhu, Y., Long, H. & Zhang, W. Imine-Linked Porous Polymer Frameworks with High Small
- Gas (H2, CO2, CH4, C2H2) Uptake and CO2/N2 Selectivity. *Chem. Mater.* **25,** 1630–1635
- 562 (2013).
- 563 24. Yeom, C. K., Lee, S. H. & Lee, J. M. Study of transport of pure and mixed CO2/N2 gases
- through polymeric membranes. *J. Appl. Polym. Sci.* **78**, 179–189 (2000).

- 565 25. Hu, G., Smith, K. H., Wu, Y., Kentish, S. E. & Stevens, G. W. Screening Amino Acid Salts as
- Rate Promoters in Potassium Carbonate Solvent for Carbon Dioxide Absorption. *Energy Fuels*
- **31,** 4280–4286 (2017).
- 568 26. Knuutila, H., Juliussen, O. & Svendsen, H. F. Kinetics of the reaction of carbon dioxide with
- aqueous sodium and potassium carbonate solutions. *Chem. Eng. Sci.* **65,** 6077–6088 (2010).
- 570 27. Knuutila, H., Svendsen, H. F. & Juliussen, O. Kinetics of carbonate based CO2 capture
- 571 systems. *Energy Procedia* **1,** 1011–1018 (2009).
- 572 28. Knuutila, H., Hessen, E. T., Kim, I., Haug-Warberg, T. & Svendsen, H. F. Vapor-liquid
- equilibrium in the sodium carbonate—sodium bicarbonate—water—CO 2 -system. *Chem. Eng.*
- 574 *Sci.* **65,** 2218–2226 (2010).

- 575 29. Carbon Dioxide Capture and Storage, Contribution of the Working Group III, Special Report
- of the Intergovernmental Panel on Climate Change. (2005).